

V. PHYSICAL ELECTRONICS AND SURFACE PHYSICS*

Academic and Research Staff

Prof. R. E. Stickney
Dr. T. Krivachy

Graduate Students

V. S. Aramati	C-N. Lu
A. E. Dabiri	D. V. Tendulkar

A. EXPERIMENTAL MEASUREMENTS OF THE SPATIAL DISTRIBUTION OF H₂ AND D₂ DESORBED FROM A NICKEL SURFACE

1. Introduction

It is usually assumed that molecules desorbed from a solid surface will have a Maxwellian velocity distribution with temperature equal to that of the solid.¹ As a consequence, it is generally expected that the spatial distribution of desorbed molecules will be diffuse, that is, proportional to $\cos \theta$, where θ is the angle of inspection measured from the surface normal. Recently, however, van Willigen² and Palmer et al.³ have reported experimental data showing that the spatial distributions of hydrogenic molecules (H₂, D₂, HD) desorbed from nickel deviate markedly from $\cos \theta$. These data show that the desorbed molecules are more highly concentrated along the surface normal than is predicted by the $\cos \theta$ relation.

Since molecular desorption processes are encountered in a variety of technological problems (catalysis, high-temperature oxidation, degassing of metals), we believe that it is important to attempt to establish a theoretical model that successfully explains these phenomena. To aid in the development of this model, we plan to measure the velocity distribution of H₂ and D₂ molecules desorbed from nickel single crystals that are cut so as to obtain surfaces corresponding to three different crystallographic orientations, for example, the (100), (110), and (111) orientations. The apparatus constructed for these measurements has been described in a previous report.⁴ We have also developed a much simpler apparatus for measuring spatial distributions in a manner similar to that reported by van Willigen.² This apparatus will be described, and some preliminary data on the desorption of H₂ and D₂ from a polycrystalline Ni surface will be reported and discussed in detail.

*This work was supported principally by the National Aeronautics and Space Administration (Grant NGR 22-009-091), and in part by the Joint Services Electronics Programs (U. S. Army, U. S. Navy, and U. S. Air Force) under Contract DA 28-043-AMC-02536(E).

(V. PHYSICAL ELECTRONICS AND SURFACE PHYSICS)

2. Experimental Apparatus and Procedure

The principal components of the apparatus are shown in Fig. V-1. One side of the Ni membrane is exposed to H_2 (or D_2) at approximately atmospheric pressure, while the other side is exposed to vacuum. Hydrogen atoms diffuse through the membrane and recombine on the surface to form molecules that desorb into the evacuated chamber. The spatial distribution of the molecules desorbing from the membrane is measured by a conventional ionization gauge mounted on a rotatable shaft whose center line is tangential to the membrane surface at its center.

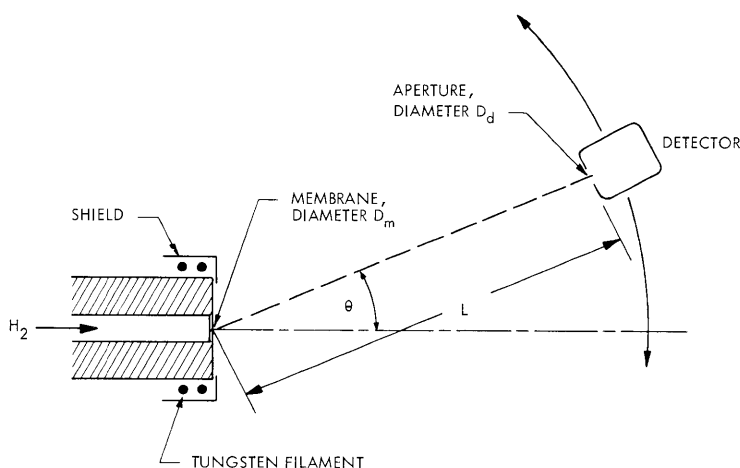


Fig. V-1. Experimental apparatus for measurements of spatial distribution.

The membrane was formed at the end of a rod of polycrystalline nickel (Grade A, International Nickel Co.), 1.27 cm in diameter, by boring a hole, 0.6 cm in diameter, to obtain the desired membrane thickness. In the present case, the thickness was $l \approx 0.25$ mm after the surface was mechanically polished. The membrane assembly is mounted at the end of a tube that passes through the chamber wall to a valve and on to a flask of Research Grade H_2 . This tube is evacuated before filling it with H_2 to a pressure of ~ 1 atm.

The membrane assembly is heated by electron bombardment from a hot tungsten filament (Fig. V-1). A bombardment current of ~ 0.4 A at 300 V is sufficient to maintain the membrane at 1500°K , which was selected as the maximum temperature in the present experiment. (Nickel melts at 1725°K .) The temperature is measured with a chromel-alumel thermocouple (0.254-mm diameter wire).

The vacuum chamber is a stainless-steel cylinder, 46 cm diameter, evacuated by a 500 liter/s Varian ion pump. According to the manufacturer,⁵ the pumping speed should

(V. PHYSICAL ELECTRONICS AND SURFACE PHYSICS)

be $\sim 1,350$ liter/s for H_2 . Since copper gaskets are used in all flanges, the entire system may be baked. Although it was possible to attain pressures of the order of 1×10^{-10} Torr, in the present study we generally began an experimental run when the pressure reached $\sim 1 \times 10^{-9}$ Torr.

The detector is a Varian ionization gauge (Model UHV-12P) with a glass envelope to which we have connected a kovar tube, 2.54 cm in diameter. In the present experiments, the diameter of the aperture (Fig. V-1) in this tube is $D_d = 0.3$ cm, and the distance from the center of the membrane to the detector aperture is $L = 5$ cm. By mounting the detector on an arm connected to the shaft of a rotary-motion feed-through, it is possible to vary θ from -90° to $+90^\circ$. The detector is connected to a conventional ionization gauge controller (Varian Model 971-0014), with the exception that the signal from the ion collector is read on a Keithley Model 150A electrometer. The zero-suppress feature of this electrometer allows us to cancel the signal arising from the background gas in the chamber. We observed that electron bombardment of the membrane produced anomalous changes in the detector output signal, but it was possible to eliminate this effect by biasing the kovar tube negative with respect to the tungsten filament that was the source of the bombarding electrons.

The rate of permeation of hydrogen through a nickel membrane of thickness ℓ (mm), area A_m (cm^2), and at temperature T ($^\circ K$) may be predicted from⁶⁻⁸

$$R \left(\frac{\text{molecules}}{\text{sec}} \right) = \frac{3.75 \times 10^{17}}{\ell} A_m \left(p_1^{1/2} - p_2^{1/2} \right) \exp \left(- \frac{13,900}{R_o T} \right), \quad (1)$$

where p_1 and p_2 are the H_2 pressures (Torr) on the high- and low-pressure sides of the membrane, and R_o is the universal gas constant. In the present case, $p_1 \approx 760$ Torr, $p_2 \approx 0$, $A_m = 0.28$ cm^2 , $\ell = 0.25$ mm, so

$$R \approx 1.2 \times 10^{19} \times 10^{-3,030/T}. \quad (2)$$

Therefore, $R \approx 1.9 \times 10^{15}$ molecules/s at $800^\circ K$, and it rises to 5.6×10^{16} at $1300^\circ K$.

If we assume for the present that the spatial distribution of the desorbed molecules is proportional to $\cos \theta$, then the flux of molecules within solid angle $d\omega$ is given by

$$\Gamma = \frac{1}{\pi} R \cos \theta d\omega. \quad (3)$$

(Note: Since this expression is derived by assuming that the membrane may be treated as a point source, it is not strictly valid in the present case. The derivation of a more exact expression will be outlined.)

The solid angle accepted by the detector aperture is approximately equal to A_d/L^2 , where A_d is the aperture area, and L is the distance from aperture to membrane.

(V. PHYSICAL ELECTRONICS AND SURFACE PHYSICS)

Therefore, the flux into the detector is

$$\Gamma = \frac{RA_d}{\pi L^2} \cos \theta. \quad (4)$$

This flux will cause the pressure of H_2 in the detector to increase to the point where the flux out of the detector, Γ' , becomes equal to the flux in, Γ . This outward flux may be expressed as

$$\Gamma' = \Delta p_d A_d (2\pi mkT_d)^{-1/2}, \quad (5)$$

where Δp_d is the pressure increase attributable to Γ , m is the molecular mass of H_2 , k is Boltzmann's constant, and T_d is the temperature of the gas in the detector. Equating Eqs. 4 and 5 and solving for Δp_d , we obtain

$$\Delta p_d = (2\pi mkT_d)^{1/2} \frac{R}{\pi L^2} \cos \theta \quad (6a)$$

$$\approx 1 \times 10^{-23} R \cos \theta, \quad (6b)$$

where it is assumed that $T_d \approx 373^\circ K$, and $L = 5$ cm. With the aid of Eq. 2 for R , it is possible to predict that the values of Δp_d corresponding to membrane temperatures of 800° and $1300^\circ K$ are $\sim 2 \times 10^{-8}$ and $\sim 6 \times 10^{-7}$ Torr, respectively, for $\theta = 0^\circ$.

If we assume that permeation through the side walls of the membrane assembly is negligible, then Eq. 2 represents the total flow of molecules into the vacuum chamber. This flow causes the chamber pressure to increase to the point where the pump can handle the additional gas load. That is, the increase in chamber pressure, Δp_c , is given by

$$\Delta p_c = R/S \quad (7a)$$

$$\approx 2.7 \times 10^{-4} \times 10^{-3,030/T}, \quad (7b)$$

where Eq. 2 has been substituted for R , and the pumping speed, S , is assumed to be 4.5×10^{22} molecule/Torr-s (1,350 liter/s). Therefore, the predicted values of Δp_c for membrane temperatures of 800° and $1300^\circ K$ are $\sim 4.2 \times 10^{-8}$ and $\sim 1.2 \times 10^{-6}$ Torr, respectively.

The total pressure in the detector, p_t , is equal to the sum of Δp_d , Δp_c , and p_r , the residual pressure ($\sim 1 \times 10^{-9}$ Torr). Since the output signal from the detector is proportional to p_t , we see that the desired information (Δp_d) is superimposed on a background signal ($\Delta p_c + p_r$) which should be independent of θ . According to the values computed above, the magnitude of Δp_d at $\theta = 0^\circ$ is approximately a factor of two

smaller than the background signal for reasonable values of the membrane temperature. The zero-suppress feature of the electrometer allows us to cancel the background signal which is measured by rotating the detector to $\theta = 90^\circ$.

3. Experimental Results

Shown in Fig. V-2 are the spatial distributions of H_2 measured at two different values of the membrane temperature, 863°K and 1268°K . Notice that the experimental data deviate substantially from the $\cos \theta$ relation, and, in both cases, it appears that the data fall close to the curve corresponding to $\cos^4 \theta$. Distributions were obtained at a number of membrane temperatures in the range 863° to 1268°K , and in all cases the normalized data were essentially identical to those shown in Fig. V-2. We conclude that the shape

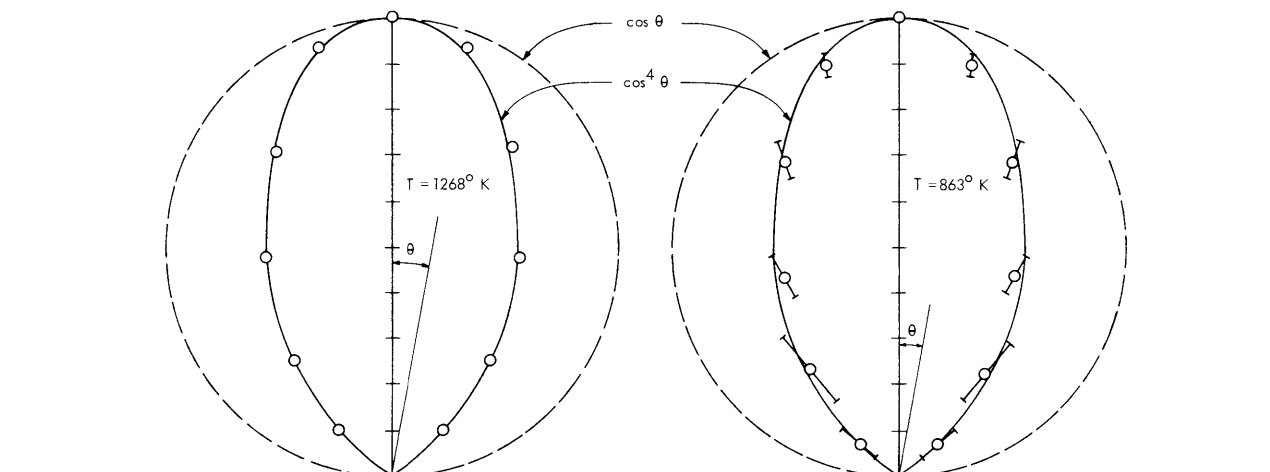


Fig. V-2. Spatial distributions of H_2 desorbed from a polycrystalline Ni surface at two temperatures, 1268°K and 863°K . For $T = 1268^\circ\text{K}$, the measured values of Δp_d ($\theta = 0$) and Δp_c are 1.9×10^{-6} and 9×10^{-6} Torr; the corresponding values for $T = 863^\circ\text{K}$ are 1.3×10^{-7} and 9×10^{-7} Torr.

(the width at half maximum) of the distributions appears to be quite independent of temperature, and it may be represented approximately by the function $\cos^4 \theta$. Similar measurements were performed for the desorption of D_2 from the same membrane and, although the absolute magnitudes of these data were slightly higher than the corresponding data for H_2 , the normalized spatial distributions appeared to be identical. That is, the normalized data for D_2 agree closely with the $\cos^4 \theta$ relation for all membrane temperatures in the range of the present experiments.

(V. PHYSICAL ELECTRONICS AND SURFACE PHYSICS)

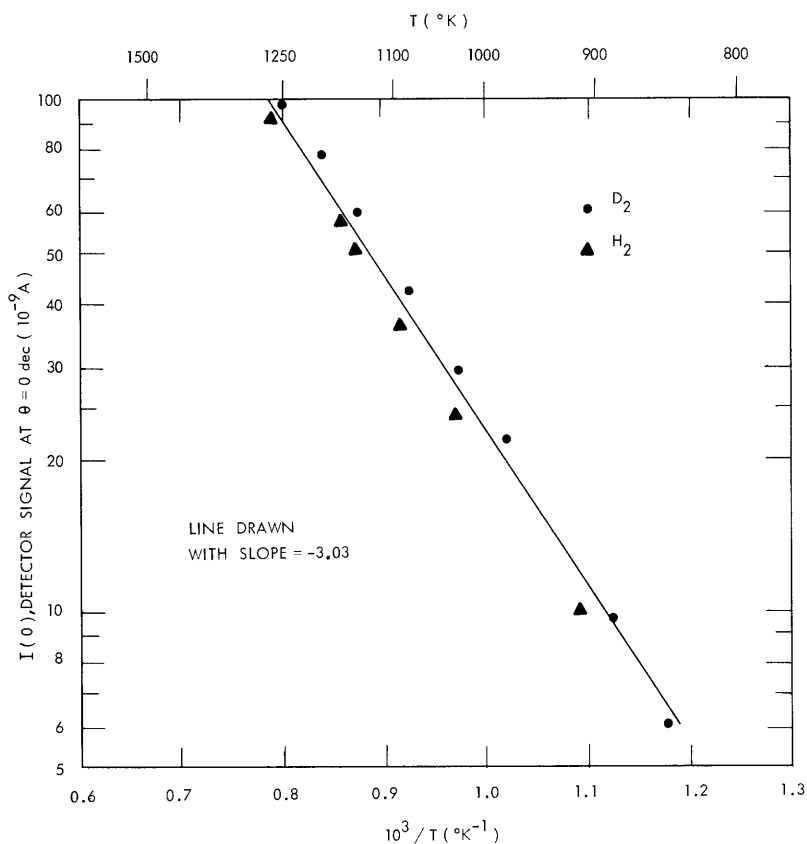


Fig. V-3. Temperature dependence of the detector signal at $\theta = 0^{\circ}$ resulting from the permeation of hydrogen through nickel.

Since the shape of the spatial distributions appears to be constant, the detector signal at any given value of θ , $I(\theta)$, should be directly proportional to the total permeation rate, R . Therefore, according to the expression for R given in Eq. 2, the slope of an Arrhenius plot of $I(\theta)$ vs $10^3/T$ should be equal to -3.03 . Data for both H_2 and D_2 are plotted in this manner in Fig. V-3 for the case $\theta = 0^{\circ}$, and we see that the slopes are very nearly equal to -3.03 . This result provides some assurance that our permeation rates are consistent with those measured by other investigators.⁶⁻⁸ If the proportionality factor between $I(\theta)$ and R were known, we could perform a more stringent test of the absolute magnitude of the present permeation rate with that reported by others (for example, Eq. 2). This would require, however, a more accurate analysis than that previously described.

4. Discussion

a. Comparison with Existing Data

Comparable data on the spatial distribution of H_2 desorbed from polycrystalline Ni have been reported by van Willigen,² but his results indicate that the approximate form

of the distribution is $\cos^9 \theta$ rather than $\cos^4 \theta$. The magnitude of this discrepancy is surprisingly large considering that the experimental techniques and temperature ranges are nearly identical. The problem is complicated further by the fact that, according to the results of Palmer et al.,³ the spatial distribution of HD desorbed from the (111) face of a Ni crystal is of the form $\cos^4 \theta$ for the most perfect crystals that they could grow. (For less perfect crystals the form was $\cos^d \theta$, with $2.5 \lesssim d < 4$.) Since we suspect that the surfaces of Palmer et al. were far smoother than the polycrystalline surface of van Willigen and ourselves, it is difficult to understand why their spatial distributions were not narrower. There are six possible explanations.

1. The value of d , the exponent in the relation $\cos^d \theta$, may depend upon the crystallographic orientation of the surface. We plan to examine this possibility by measuring the spatial distributions of H_2 desorbed from the (100), (110), and (111) crystal faces of Ni.

2. The value of d may depend strongly on the presence of impurities on the Ni surfaces. In future experiments we shall vary the composition and concentration of surface impurities (for example, carbon and oxygen) to determine if these cause the spatial distributions to change. An Auger electron spectrometer⁹ will be used to determine the composition and concentration of surface impurities.

3. The spatial distributions may be broadened by surface roughness, thereby causing the apparent value of d to be substantially less than that for a smooth surface. To examine this possibility, we shall compare spatial distributions corresponding to various degrees of surface roughness, as determined by optical and electron microscopy.

4. The geometry of the membrane and detector may cause the spatial distributions to appear broader than they actually are. (This effect is considered in this report.)

5. The molecules of the background gas in the chamber also enter the detector after being scattered from the test surface, and their contribution to the output signal may cause the apparent spatial distribution to differ from the distribution of the desorbed molecules alone. (Based on the analysis given in this report, we believe that this possibility may be disregarded in the present experiments.)

6. The value of d may vary with the coverage (concentration) of hydrogen on the Ni surface, which is a function of the permeation rate, background pressure, and membrane temperature. We believe that this possibility is not significant in the present study because our results indicate that d remains approximately constant over a wide range of experimental conditions, that is, over a range of coverages. In future work we shall determine whether the form of the spatial distributions is independent of the background pressure, which may be increased by throttling the ion pump.

(V. PHYSICAL ELECTRONICS AND SURFACE PHYSICS)

b. Geometrical Effects

Since the permeation rate is inversely proportional to thickness, we would expect the coverage of adsorbed hydrogen on the end of the membrane assembly to be greater at the center than at the edges. The distribution of coverage over the surface depends on the relative rates of surface diffusion and desorption as functions of coverage. These rates are unknown, so we have been unable to calculate the coverage distribution. Since it is known, however, that the rate of surface diffusion of hydrogen on metals is much greater than the rate of desorption, we shall assume that the coverage is uniform over the entire end of the membrane assembly. This leads to the assumption that the desorption occurs at an equal rate over the entire end of area A_e , even though permeation occurs predominantly through the thinned central portion (the "membrane") of area A_m .

Since the ratio of A_d , the area of the detector aperture, to A_e , defined above, is 0.0557 in the present case, we may consider the detector aperture to be a point relative to the test surface. That is, the broadening introduced by the finite area of the detector aperture is much less than that introduced by the test surface, which is estimated here.

To obtain a rough estimate of the possible broadening of the spatial distribution resulting from the finite area of the test surface, we shall derive an expression for the distribution of molecules desorbed from a narrow strip on the test surface that is centered about the line of intersection of the detector plane of rotation with the surface (see Fig. V-4). Although this two-dimensional approximation of the three-dimensional situation is not expected to be completely valid, it is significantly better than assuming the surface to be a point.

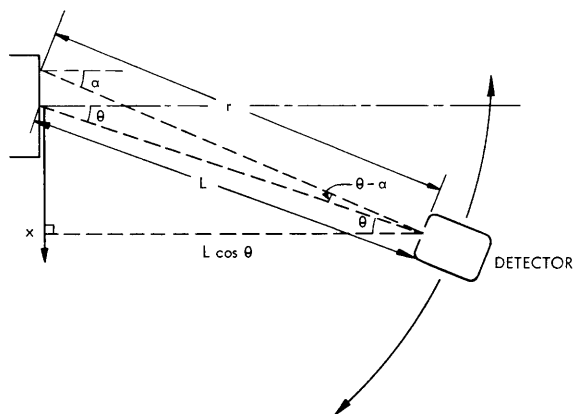


Fig. V-4. Geometry of membrane-detector configuration.

Consider a strip of infinitesimal width dy and length equal to the diameter of the test surface D_e . In terms of the symbols shown in Fig. V-4, the differential flux entering the detector from an infinitesimal area $dx dy$ at point x on the strip is

$$d\Gamma(\theta, x) = \frac{R}{\pi D_e dy} \frac{\cos a A_d \cos(\theta-a) dx dy}{r^2}, \quad (8)$$

where $R/D_e dy$ is the desorption rate per unit area, $\cos a$ is the assumed form of the spatial distribution, $A_d \cos(\theta-a)$ is the projection of the detector aperture area upon a plane perpendicular to the line between the surface infinitesimal and the aperture, and r is the length of this line. The principal geometrical relations are

$$\cos a = \frac{L \cos \theta}{r} \quad (9)$$

$$\sin a = \frac{L \sin \theta - x}{r} \quad (10)$$

$$r^2 = (L \cos \theta)^2 + (L \sin \theta - x)^2 = L^2 + x^2 - 2 \times L \sin \theta. \quad (11)$$

By substituting these in Eq. 8 and then integrating from $x = -\frac{1}{2} D_e$ to $x = +\frac{1}{2} D_e$, we obtain

$$\Gamma(\theta) = \frac{R A_d}{2\pi D_e} \left\{ \cos \theta \left[\frac{D_e (L^2 + D_e^2/4)}{(L^2 + D_e^2/4)^2 - L^2 D_e^2 \sin^2 \theta} \right] + \frac{1}{L} \left[\tan^{-1} \frac{D_e - 2L \sin \theta}{2L \cos \theta} - \tan^{-1} \frac{-D_e - 2L \sin \theta}{2L \cos \theta} \right] \right\}. \quad (12)$$

For the dimensions of the present apparatus, the denominator of the first term may be approximated by $(L^2 + D_e^2/4)^2$, since the maximum error would be less than 6%. Furthermore, the second bracketed term may be rewritten

$$\tan^{-1} \frac{L D_e \cos \theta}{L^2 - D_e^2/4}, \quad (13)$$

by employing the relation $\tan(\beta - \gamma) = (\tan \beta - \tan \gamma)/(1 + \tan \beta \tan \gamma)$. Since $L D_e \cos \theta / (L^2 - D_e^2/4) \leq 0.24$ in the present study, we may approximate Eq. 13 by

$$\frac{L D_e \cos \theta}{L^2 - D_e^2/4}, \quad (14)$$

with the maximum error being less than 2%. Therefore, Eq. 12 becomes

$$\Gamma(\theta) \approx \frac{R A_d}{\pi L^2} \cos \theta \left[\frac{1/2}{1 + \left(\frac{D_e}{2L}\right)^2} + \frac{1/2}{1 - \left(\frac{D_e}{2L}\right)^2} \right]. \quad (15)$$

(V. PHYSICAL ELECTRONICS AND SURFACE PHYSICS)

Since $D_e/2L = 0.06$ in the present case, the term in brackets is approximately unity, and Eq. 15 reduces to

$$\Gamma(\theta) \approx \frac{RA_d}{\pi L^2} \cos \theta, \quad (16)$$

which is identical to Eq. 4 which was derived by assuming the surface to be a point source. By considering the signs of the errors associated with each of the approximations underlying Eq. 16, we conclude that the over-all error will be less than the error associated with any of the separate terms, that is, less than 6%. We now plan to extend the error analysis to the case in which the spatial distribution is of the form $\cos^d \theta$.

c. Effect of Background Gas

The molecular flux entering the detector may be divided into three components: Γ , the flux of molecules desorbed from the test surface; Γ_s , the flux of background gas molecules scattered from the test surface; and Γ_b , the flux of background gas molecules that enter without being scattered from the surface, that is, those molecules not contained in the solid angle defined by the projected area of the test surface viewed from the detector aperture,

$$\omega_b = A_e \cos \theta / L^2,$$

where A_e is the area of the end of the membrane assembly. It seems reasonable to assume that the background gas is at the temperature of the chamber walls ($\sim 300^\circ\text{K}$) and that the directions of the molecules are random. Therefore, the flux of background molecules upon the test surface is

$$Z = p_b A_e (2\pi mkT_c)^{-1/2}, \quad (17)$$

where p_b is the background pressure ($p_b = p_r + \Delta p_c$), m is the average molecular mass (assumed to be the mass of H_2 , since it is the dominant component of the background gas), and T_c is the temperature of the chamber walls. If we assume that p_r is negligible relative to Δp_c , then the ratio Z/R may be expressed in the following form with the aid of Eqs. 7a and 17:

$$Z/R = \frac{A_e}{S} (2\pi mkT_c)^{-1/2}. \quad (18)$$

By substituting the appropriate values for the present study, we obtain $Z/R \approx 4 \times 10^{-2}$. Therefore, we would expect that the flux of background gas upon the test surface would have a negligible effect on the surface coverage and on the measured spatial distribution.

(V. PHYSICAL ELECTRONICS AND SURFACE PHYSICS)

If the background molecules are emitted (including both scattering and desorption) diffusely from the surface, then the sum of their contribution to the detector signal (Γ_s) plus that associated with the other background molecules (Γ_b) will constitute a signal that is independent of θ , thereby causing no distortion of the spatial distribution, regardless of the magnitude of Z/R . On the other hand, if these molecules are emitted in such a manner that their spatial distribution is broader than $\cos \theta$, then they could distort the measured distribution at large values of θ , even though Z/R is small.

A. E. Dabiri, R. E. Stickney

References

1. For a review of the literature pertaining to this problem see L. B. Loeb, Kinetic Theory of Gases (McGraw-Hill Book Company, New York, 2d edition, 1934); also see R. L. Palmer et al., Report 9701, Gulf General Atomic, December 1969.
2. W. van Willigen, Phys. Letters 28A, 80 (1968).
3. R. L. Palmer, J. N. Smith, Jr., H. Saltsburg, and D. R. O'Keefe, Report 9701, Gulf General Atomic, December 1969.
4. A. E. Dabiri and R. E. Stickney, Quarterly Progress Report No. 95, Research Laboratory of Electronics, M.I.T., October 15, 1969, p. 19.
5. Varian Instruction Manual 935-0018 (1964).
6. R. Barrer, Diffusion in and through Solids (Cambridge University Press, London, 1951), p. 168.
7. S. Dushman, Scientific Foundations of Vacuum Technique (John Wiley and Sons, Inc., New York, 2d edition, 1962), Chap. 8.
8. Y. Ebisuzaki, W. J. Kass, and M. O'Keefe, J. Chem. Phys. 46, 1378 (1966).
9. For example, see L. A. Harris, J. Appl. Phys. 39, 1419 (1968); R. E. Weber and A. L. Johnson, J. Appl. Phys. 40, 314 (1969).

